RF Shimming Capabilities at 9.4 Tesla using a 16-channel Dual-Row Array

Jens Hoffmann[1], G. Shajan[1], Klaus Scheffler[1,2], and Rolf Pohmann[1]

[1]*High-Field Magnetic Resonance Center, Max Planck Institute for Biological Cybernetics, Tuebingen, Baden-Wuerttemberg, Germany,* [2]*Department for Biomedical Magnetic Resonance, University of Tuebingen, Tuebingen, Baden-Wuerttemberg, Germany*

Introduction: In this work, we present a numerical and experimental investigation of the RF phase shimming capabilities at 9.4 Tesla using an inductively decoupled, 16-channel dual-row array for human brain imaging.

RF transmit arrays that are designed in multiple rows are a relatively new development for human neuroimaging at ultra-high fields, especially at 9.4 Tesla [1, 2]. These arrays offer improved coverage in z-direction along with the capability to control the B_1^+ field in all spatial dimensions. With static RF shimming, this can be used to trade B_1^+ homogeneity against power efficiency in arbitrary brain volumes, depending on the desired application. However, to assess local SAR as function of input power and RF shim settings, numerical simulations must be provided that realistically incorporate the relevant details of the RF setup, including the array's input and decoupling networks.

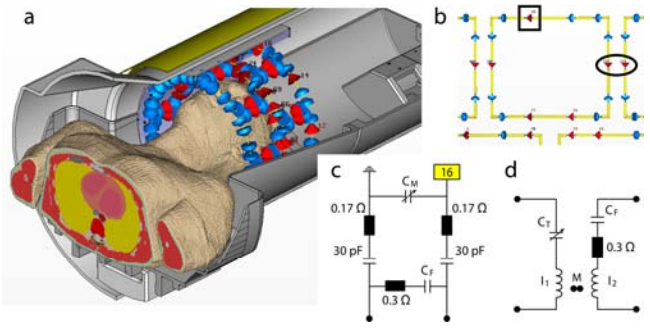

Fig. 1: Simulation setup in 3D domain (a). Single loop (b) with fixed capacitors (blue arrows) and ports (red arrows; square: input, circle: decoupling). Input and inductive decoupling networks are realized in circuit domain as shown in (c) and (d), respectively.

Methods: Experiments were conducted on a 9.4 T whole-body MR scanner (Siemens, Germany) equipped with an AC84 head gradient insert. Construction details of the dual-row transmit array are given in [1]. RF shimming is described in [3] and was based either on measured or simulated single-channel B_1^+ maps. Time-domain simulation together with circuit co-simulation was performed using CST Studio Suite (CST, Darmstadt, Germany). The RF setup in 3D domain contains a precise model of the dual-row array and the relevant scanner interior (Fig.1a). Realistic electrical properties were assigned to all materials and a series resistance was added to each fixed capacitor to account for component losses. The input/decoupling circuits were replaced by 50 Ohm ports (Fig 1b, 80 ports in total) and modeled in circuit domain as shown in Figs.1c and 1d.

Results: After adjustment of the coil model, a good match between simulated and experimental B_1^+ patterns, S-parameters, decoupling inductances and tuning/matching capacitances was obtained. However, the B_1^+ level in the experiment was about 25 % lower than in simulation for the same input power, indicating additional losses. Interestingly, the simulation tool predicts that about one third of the input power is dissipated in the capacitors and only about 45 % is actually dissipated in biological tissue.

Fig. 2 shows simulated B_1^+ maps in CP mode and after slice-by-slice B_1^+ shimming with focus either on the removal of field voids or on homogeneity [1]. Numbers below the images give the min/mean/max B_1^+ field [nT/V], inhomogeneity [%] and safety excitation efficiency (SEE [4], [µT/sqrt(W/kg)]). Compared to the CP mode, the "no voids" solution usually lifts the lowest field values considerably and even improves field uniformity. Inhomogeneity in the order of 10% can be achieved when shimmed for homogeneity, but often with a 50% drop in efficiency. This in turn limits SEE, i.e. the allowed B_1^+ level with respect to local SAR. RF shimmed MR images are shown in Fig. 3. Efficiency and homogeneity were balanced to create sufficient B_1^+ in order to reach high flip-angles (FA) using the vendor-provided TSE sequence (Fig. 3a, b) or to limit the B_1^+ variation to a range of about 1:2 for proper adiabatic spin inversion in the MP2RAGE sequence (Fig. 3c). For these images, the transmit array was combined with a 31-channel receive-only array [5].

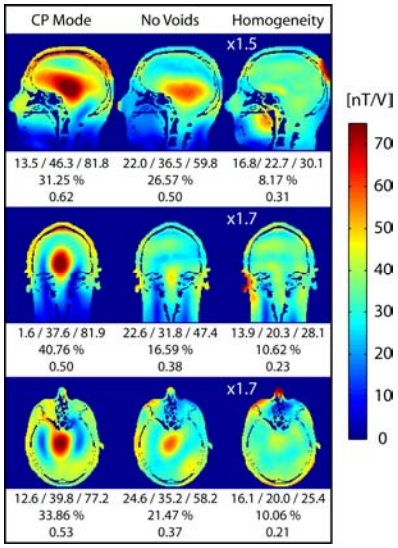

Fig.2: Simulated field maps along with in-slice B_1^+ field statistics and SEE. B_1^+ in homogeneous solutions is scaled by the indicated factors for better visualization.

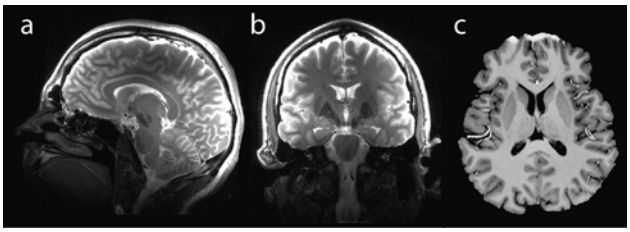

Fig.3: RF shimmed TSE (a, b) and MP2RAGE (c) images. TSE with TR/TE = 6000/46 ms, GRAPPA = 2, Turbo Factor = 11, resolution = 0.6x0.6x1.5 mm, acq. time < 2 min. MP2RAGE: $TR/TI_1/TI_2$ = 8.5/1.2/3.7 s, nominal FA = 4°/5°, resolution = (0.8x0.8x1) mm³, inversion pulse: 13 ms non-selective TR-FOCI.

Discussion: The dual-row design provides RF shimming in all spatial dimensions in order to trade off homogeneity and max-to-min ratio against power-efficiency and SEE. This enables uniform low FA imaging as well as certain B_1^+ sensitive high FA applications at 9.4 T. In contrast to our previous simulations [1], consideration of the input/decoupling circuitry allows for quantitative comparison of simulated and measured results and an assessment of the power budget. Precise simulations will be of increasing importance to fully utilize pTx techniques since local SAR supervision will be based on customer-provided models in many next-generation pTx systems. However, future work must investigate the remaining discrepancy between the B_1^+ levels in experiment and our preliminary simulations.

References: [1] G. Shajan et al. ISMRM 2012, #308; [2] Felder et al. ISMRM 2012, #2609, [3] Hoffmann et al. ISMRM 2010, #1470; [4] Kozlov and Turner, 33rd IEEE EMBS 2011, 547–553; [5] G. Shajan et al. ESMRMB 2012, #351.